# APERTURE COUPLED MODIFIED RECTANGULAR DIELECTRIC RESONATOR ANTENNA ARRAYS FOR X-BAND APPLICATIONS

SOVAN MOHANTY[*], BAIBASWATA MOHAPATRA

School of Electrical, Electronics and Communication Engineering, Galgotias University, Greater Noida 201310,

India

**Abstract:** This paper proposes an aperture coupled 3×3 rectilinear geometry-based periodic modified rectangular dielectric resonator antenna array for X-band applications. In this paper, the complex electromagnetic field problem of RDRA is addressed through a modified rectilinear-shaped DRA. Notches are created on the dielectric resonator to alter the normal components of the electric field pattern instantaneously. It leads to the reduction in the magnitude of reactive current density, resulting in a lessening of the Q-factor and enhancement of the bandwidth. This antenna shows multiband response, resonating at 8.42, 10.08, and 11.60 GHz frequency with a peak gain of 12.94 dBi at 9.75 GHz with consistent gain stability over the entire frequency band of operation. The radiation efficiency is around 96.1% due to low losses. The impedance bandwidths for different bands are 4.51%, 2.77%, and 4.56% at the resonating frequency of 8.42, 10.08, and 11.60 GHz. A comparative analysis of input and output characteristics is carried out between single, double, and nine-cell arrays. The designed antenna is excited by a branch line series-corporate constrained micro-strip feeding network with three apertures. This novel design is suitable for microwave X-band applications.

[*]Corresponding author

E-mail address: mohanty.sovan@gmail.com

## 1. INTRODUCTION

Richtinger has developed a microwave resonator, in the form of a dielectric sphere and toroid, in 1939, Richtinger [1]. The output field patterns of the dielectric resonators were initially studied by Okaya and Barash [2]. The dielectrics with conducting shields were used as a resonator in the amplifier and oscillator circuit. With the opening of the conducting shield and by varying parameters like aspect ratio, dielectric constant, and the feeding mechanism, the dielectric resonator can become an efficient radiator. DRA shows good electrical characteristics, but non-electrical behavior like low profile, miniaturized and conformal design makes it suitable for integration with modern microwave integrated circuits. It has high power handling capability, high gain, high radiation efficiency, and low feed network losses. DRA technology will prove to be a viable alternative to the more established microstrip patch antenna technology. At microwave and millimeter-wave frequency of operation, the performance of the microstrip patch antenna degrades due to high ohmic losses, dielectric losses in the patch, and the feed network. The parasitic radiation of surface wave in the dielectric substrate dominates, Luk and Leung[3] In a dielectric, displacement current are approximately a hundred times more than that of conduction current. Because of the low displacement current density, the gain is low with a broad radiation pattern.

To enhance the effective gain, the directivity of a dielectric resonator antenna, unit cells can be arranged in an array format. An array is the electrical and geometric arrangements of the unit cells that provide enhanced electric and magnetic field intensity in the desired direction. The radiation performances improve by adjusting the number of radiators, their locations, feeding techniques, and mutual coupling, Petosa [4]. The amplitude and phase of the impressed current of the source play a crucial role in the beam pattern, Petosa [5]. The phase angle of the impressed

current from the source controls the output peak of the beam, and amplitude reduces the sidelobe levels, Petosa [6]. The unwanted grating lobe can be mitigated by increasing the radiator, particularly at the edge, to improve the scan angle, Hussain, Sharawi, Podilchack, and Antar [7]. The potential hazard lies in impedance and pattern inconsistencies lead to scan blindness. It occurs at a certain scan angle where input impedance enters into a mismatch condition, Petosa [8]. Therefore, instead of the generation of forwarding traveling waves from the source to the antenna, standing wave dominates to empower the reactive power. The near field components dominate that of the far-field. The scan blindness is a function of mutual coupling, Jones, Chow, Sheeto, Petosa and Thirakoune [9, 10].

In this paper, a 3×3 aperture coupled modified rectangular dielectric resonator antenna array is proposed. A rectilinear DR structure is designed and modeled from the core rectangular geometry as the base. Notches are created on the surface, which is responsible for altering the electrical field distribution instantaneously. The gap created by the notches is perpendicular to the electric field pattern. Therefore, the electric field present within the notches will get boosted up after excitation through proper modes. It will change the resonant frequency and the radiation Q-factor, Mongia, Bhartia, [11]. This nine elements modified dielectric resonator antenna provides a multiband response, resonating at 8.42, 10.08, and 11.60 GHz frequency with the minimum surface wave and dielectric losses. FEM technique is preferred as it does not require any formulation of equivalent current. Rectilinear-shaped complex geometries can be analyzed by using FEM computational technique, Harrington [12]. Here, HFSS (High-Frequency Structural Simulator) based on FEM (Finite Element Method) is used as a 3-D electromagnetic tool for the simulation. Finally, a comparative analysis is made between single, double, and nine-unit cells to form an array.

This paper highlights the configuration, performance, and challenges associated with the proposed design. The principle of operation of the array configuration is presented in Section II. The structure of the antenna is described in Section III. Detailed result analyses and discussions are presented in Section IV. Finally, conclusions are given in Section V.

## 2. PRINCIPLE OF OPERATION

Each unit cell of the modified rectangular dielectric resonator antenna can be arranged in an array format to enhance directive gain and desired radiation pattern. Decoupling of the terminal characteristics impedance and the radiation pattern is crucial. Maximum directivity can be achieved through a linear phase progression of each element, Loos, Anter [13]. The array pattern of N-identical elements is the function of the radiation intensity of the unit cell and the array factor. Array factor is the radiation pattern obtained when each unit cell radiates isotropically.

$$AP = 20 \log_{10}(EP.AF) \tag{1}$$

where, AP is the array pattern, EP is the radiation intensity of each element (Emission pattern), and AF is the array factor. The general equation of array where arrays are placed randomly is [4]:

$$AF = \sum_{n=1}^{N} A_n e^{j\psi_n} = \sum_{n=1}^{N} A_n e^{jnk_0} \tag{2}$$

Phase $(\psi_n) = k_0 x_n \sin\theta \cos\emptyset + k_0 y_n \sin\theta \sin\emptyset$

General equation of array geometry for evenly spaced array is [4]:

$$AF = \sum_{n=1}^{N} A_n e^{jnk_0 d \sin\theta} \tag{3}$$

where, $k_0 = 2\pi/\lambda_0$ and the free space wave length $\lambda_0$, and $A_n e^{j\beta_n}$ is the complex voltage excitation. For a rectangular lattice of 3×3 elements, when elements are placed at a distance of $dx$ and $dy$ in the x and y direction respectively, then array factor will be:

$$AF = [A_0 \sin(3\,\psi_x/2) \sin(3\,\psi_y/2)]/[\sin(\psi_x/2) \sin(\psi_y/2)] \tag{4}$$

where, $\psi_x = k_0 d_x \sin\theta + \beta_x$, $\psi_y = k_0 d_y \sin\theta + \beta_y$, $\beta_x = -k_0 d_x \sin\theta_0 \cos\emptyset_0$, and $\beta_y = -k_0 dy \sin\theta_0 \sin\emptyset_0$

Equation (4) is valid under the unloaded condition. It is considered that there is the presence of a large number of uniform array elements, and each element is facing almost similar types of environment. The total array structure is placed over the infinite ground plane. However, in the loaded condition and mutual coupling, the output pattern will change drastically along with the frequency behavior of the input impedance. A series corporate constrained micro-strip feeding network based on a resonant approach is used. Feed network provides a tradeoff between bandwidth and radiation efficiency. Micro-strip feed lines are terminated in the open circuit to

form the standing wave which is acting as a stub to neutralize the reactive components. While providing impedance matching, it is required to adjust the resistance and reactance until the absence of the standing wave. Impedance matching of multiple junctions will couple maximum energy from the feeding network to the modified RDRA through the aperture. Further DRA element can be positioned at $m\lambda_g/2$ from the open end, Petosa, Itipiboon, Anter, Roscoe and Cuhahi[14, 15].

The rectangular shape DR is the most versatile as it provides a second degree of freedom, Mohanty, Mohapatra [16]. A fixed value of multiple dimensions of RDRA can satisfy the same resonant frequency and radiation Q- factor. Under the influence of notches, the dielectric constant will depend upon the location within a volume. There will be an interaction between the original field and the generated disturbed field. If the disturbed field can be approximated well then the resonant frequency of the modified DR structure will be, Chang [17]:

$$f_r = \frac{1}{2\pi}\left[\left(\frac{W_m+W_{eb}}{W_m+W_{ea}}\right)2\pi f_0 - \frac{j\iint(H\times E_0{}^*+H_0{}^*\times E)}{W_m+W_{ea}}\right] \tag{5}$$

Where, $f_0$ is the resonant frequency of the rectangular structure before the creation of notches, $E_0$ and $H_0$ is the electric and magnetic field in a dielectric resonator.

$$W_m = \iiint \mu H_0^*.H\,d\tau$$

$$W_{ea} = \iiint \varepsilon(r)E.E_0^*\,d\tau$$

$$W_{eb} = \iiint \varepsilon E_0^*.E\,d\tau$$

Here b is the major axis of the waveguide and a is the minor axis of the waveguide. The introduction of air dielectric interface gap is perpendicular to the y-axis. An infinite ground plane is placed over the top of the substrate and it is behaving as a perfect electrical conductor except at those points where slots are created to couple the energy from the microstrip feed line to the radiator. The field structure of the PEC can be described by:

$$n \times H = J_s \text{ and } n \times E = 0 \tag{6}$$

At the boundary of a perfect electrical conductor there are vanishing tangential components of the electric field. Therefore field will lie perpendicular to the ground plane (x-y plane). There is

generation of $TE_{111}^x$ mode as the lowest order mode. The higher order modes will be $TE_{112}^x$ and $TE_{113}^x$. Further, through ground plane image theory can be applied to realize the volume of the air gap to form a loop. Here air-dielectric interface is treated as perfect magnetic conductor because $\varepsilon_r$ of Rogers RO3210(tm) = 10.2, which is much greater than that of air. In a perfect magnetic conductor, tangential components of the magnetic field is zero. The PMC approximation is applied on the surface of the RDRA and total reflection is in y-direction. The resonant frequency of the dominant mode $TE_{111}^x$ can be obtained by solving the transcendental equation under no load condition, Mongia, Ittipiboon [18]. Initially the dimension of RDRA is calculated from the dielectric waveguide model. In DWM, dielectric is treated as a part of dielectric waveguide truncated in the direction of propagation. The radiation distribution is indicated by DWM equation, Petosa [4].

$$k_x \tan\left(\frac{k_x d}{2}\right) = \sqrt{(\varepsilon_r - 1){k_0}^2 - {k_x}^2} \tag{7}$$

Where, $k_0 = \frac{2\pi}{\lambda_0} = \frac{2\pi f_0}{c}, k_y = \frac{\pi}{w}, k_z = \frac{\pi}{b},$

$$k_x = \sqrt{\varepsilon_r {k_0}^2 - {k_y}^2 - {k_z}^2} \tag{8}$$

The transcendental equation can be solved for selected ratio of w/b as a function of d/b w.r.t normalized frequency F. Here a is the major axis, b is the minor axis, and d is the length of the dielectric waveguide. The normalized frequency F can be defined as

$$F = \frac{2\pi w f_0 \sqrt{\varepsilon_r}}{c} \tag{9}$$

Here $f_0$ is the resonant frequency. The value of the normalized frequency F can be determined from the F vs. (d/b) plot for different value of (w/b). The above equation can be effectively written as

$$f_{GHz} = \frac{15F}{w_{cm} \pi \sqrt{\varepsilon_r}} \tag{10}$$

Where, resonant frequency is represented in GHz scale and w is in cm.

The gap between unit cell on the top of the ground plane will behave as inhomogeneous DR with permittivity $\varepsilon'$ as a.c. capacitivity. Therefore field within the DRA and air gap satisfy the air-dielectric continuity condition. The field within the engraved notch is very complicated and

hybrid in nature. However it is observed that due to the presence of infinite ground plane $E_x$ component will dominates over other field patterns. The notch will enhance the $E_x$ component further to satisfy the continuity condition. The output radiation pattern is strongly depend upon the   tangential electric field components on the DR surface. While operating as a transmitting array structure, power radiated by each element is affected by the surrounding field behavior. Whereas while operating as a receiving array structure, scattered power from all the nearby array elements contributes to the total power gain. This cross-relation between all the array elements is called mutual coupling. The factors which contribute to the mutual coupling are (i) the antenna element and parameters like gain, self impedance; radiation patterns (ii) the relative physical and electrical position of the element (iii) the transmission line distribution network.

## 3. ANTENNA GEOMETRY

The structure of the proposed 3×3 DRA array is shown in fig. 1and fig. 2. There are nine unit cells placed in a rectangular pattern with approximately half wavelength ($\frac{m\lambda_g}{2}$) spacing between adjacent elements. To eliminate the grating lobe in the radiation pattern, element spacing (s) has to be restricted to as per the equation (9).

$$\left(\frac{s}{\lambda_0}\right) \leq \frac{1}{1+|\cos(\theta_m)|} \tag{11}$$

Where, $\theta_m$  is the beam peak angle measured from the plane of the array. A central element in each row is fed through a narrow transverse slot to achieve linearly polarized radiation in a broadside z-direction. The branch line series corporate feed network architecture is optimized experimentally by reducing insertion loss, mismatch loss, and surface wave loss to provide almost equal divided power to each cell at the design frequency of 11.3 GHz. A substrate of length 70mm, width 70 mm and height 0.6 mm, made up of Arlon 25N (tm) having permittivity $\varepsilon_r = 3.38$   and loss tangent of 0.0025. The top of the substrate is covered with a ground plane as a perfectly electrical conductor (PEC), Wang, Zhang, Sun, Zhao [19]. Because of this main radiation pattern is being shielded from the feed network. The rectilinear shaped RDRA is made up of Rogers RO3210(tm)

having permittivity $\varepsilon_r$ = 10.2, dielectric loss tangent= 0.003. The antenna has a length (d) = 10.6 mm, width (w) = 10.6 mm and height (h = b/2) = 7.89 mm. The length, width, and height of the DRA are calculated by solving the antenna transcendental equation as described in the equation (7). As shown in fig.1 notches are engraved as per the detailed dimensions shown in the figure. To remove the problem of crowding of the feed network three apertures are placed just below the center of the unit cell in each column of 3×3 architecture. The aperture at the top of the ground plane will behave as a short dipole to initiate the back radiation, Anter, Fan [20]. Aperture is behaving as an open circuit stub. Here back radiation due to the aperture is being controlled by reducing the number of apertures for energy coupling. Coupling to RDRA is established through an equivalent magnetic current in line with the length of the slot. The unit cell is being excited by its lowest order field pattern mode $TE^x_{\delta 11}$. While designing this structure care has been taken to achieve critical coupling, excitation of lowest order mode, and proper matching to maximize the energy transfer and resonance at desired frequency, Yaduvanshi, Parthasarathy [21].
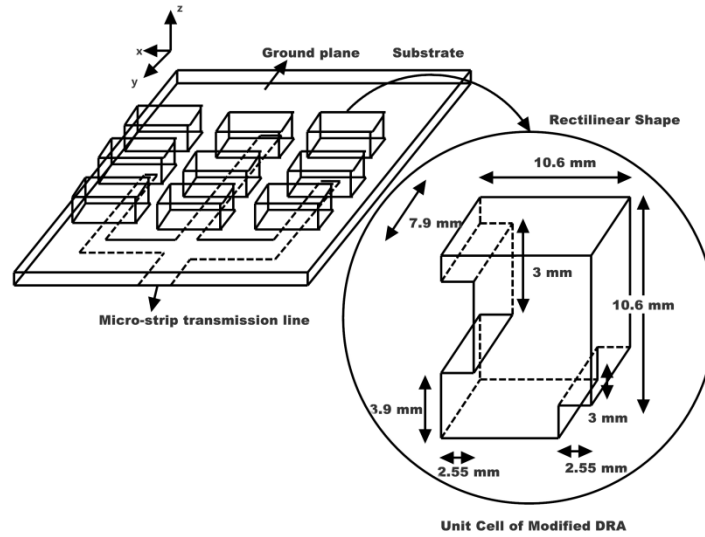


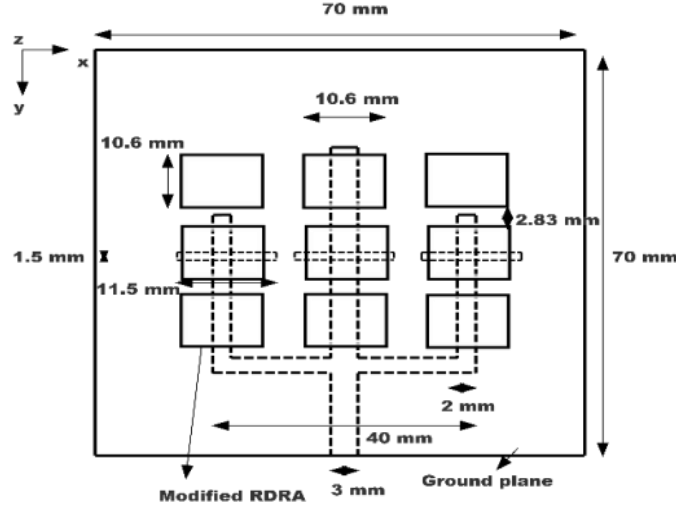Fig. 1: Side view of the proposed antenna array highlighting the structure of the unit cell

Fig. 2: Top 2-D view of the proposed antenna.

Because of geometrical complexities modified RDRA uses an insufficient and un-matured numerical technique for its performance analysis. It is required to improve RDRA's mathematical modeling to analyze its design characteristics with high accuracy. The radiation field can be evaluated from the accurate knowledge of displacement current on the antenna and the corresponding boundary condition. Entire volume, including the airbox, is discretized to solve the unknown current coefficient. The magnetic potential functions (A) can be determined from the surface current density J and the contribution of all the modes present within the device. The radiated electric (E) and magnetic field (H) will be calculated by using, Harrington [12]:

$$E = -j\omega\mu A + \frac{1}{j\omega\varepsilon}\nabla(\nabla.A) \tag{12}$$

$$H = \nabla \times A \tag{13}$$

**Table 1: Parameters of the 3×3 DRA array**

| Structural and input Parameters | Value |
| --- | --- |
| Substrate | 70×70×0.6 mm$^3$ |
| Resonant frequency | 8.42, 10.08 & 11.60 GHz |
| No. of RDRA | 9 in a 3×3 Array format |
| Total length of the array DRA | 36.23 mm |
| Total width of the array DRA | 49.2 mm |
| Characteristics impedance of the connecting line | 50 Ω |
| Length of the unit DRA | 10.6 mm |
| Width of the unit DRA | 10.6 mm |
| Height of the unit DRA | 7.89 mm |
| Impedance bandwidth | 4.51%,2.77% and 4.56% |

## 4. RESULTS ANALYSIS AND DISCUSSION

Fig. 3 shows the comparative analysis of the reflection coefficient as the input characteristics of a single unit cell, double unit cell, and 3×3 RDRA array. The return loss ($S_{11}$) corresponds to the input impedance and it is the ratio of the reflected wave phasor to the incident wave phasor. The unit cell of the RDRA is resonating in two bands with resonating frequencies of 9.48 and 10.34 GHz. The proposed 3×3 antenna array is multiband in nature. It is resonating at 8.42, 10.08, and 11.60 GHz with 10 dB return loss impedance bandwidth of 4.51%, 2.77%, and 4.56% respectively. The upward frequency shift and improvement in impedance bandwidth occur in the array due to mutual coupling between unit cells. The resonant frequency can be estimated with high degree of accuracy when field within the notch can be predicted with certain accuracy. The used slot as feeding element is inductive in nature. The stub is used to fine tune the design. The electromagnetic source is present away from the aperture to prevent higher order evanescent modes from reaching the source. Fig. 4 plots the VSWR as a ratio of the max. to the min. voltage at particular instant of time. The feeding network is an open-circuited line, which will create a standing wave to block various losses. As shown in the plot below the VSWR curve of the 3×3 array, at frequencies 8.42, 10.08, and 11.60 GHz there is a smaller reflected wave and smaller maximum and minimum of the voltage standing wave. High VSWR contributes standing wave losses on the line between the stub and the load. The desired gain can be achieved by varying the amplitude and phase of the element excitation. Amplitude is used to reduce the sidelobe level, whereas phase controls the peak of the beam. The gain does not count the losses due to polarization, impedance mismatches, and the device to which antenna is being connected. Fig.5 shows the rectangular plot of gain versus frequency of a single unit cell, double unit cell, and 3×3 RDRA array. It is observed that in a single unit cell RDRA there is a peak gain of 8.59 dB which increases to 12.94 dB by having a 3×3 RDRA array. Thus peak gain increases by around 4.35 dB. There is gain stability for the entire desire range of frequency. Fig. 6, 7, 8 (a, b, c) shows the radiation pattern along E and H plane, co and cross polarization of the unit cell, two cells, and 3×3 array antenna with the dimensions described in fig. 1 & 2. The overall maximum co-planar gain at

broadside is 12.94 dB at 11.3 GHz.

The power radiated from each element will have some scattering effect on the overall radiation pattern. The radiation pattern is deeply influenced by the microstrip line, presence of discontinuities, reflected radiation from the electrical wall formed by the ground plane, edges of the transmission line and the DRA, Shalaby, Sherbiny [22]. Here arrays are aligned in such a fashion that magnetic dipoles are both collinear and side by side. To achieve maximum coupling, the typical separation range (s) between elements is 0.5 $\lambda$. The Co and cross-polarization level of E and H plane is shown in Fig.12 & 13. The difference between E plane Co and cross-polarization is about -20 dB in the broadside direction, whereas in H-plane cross-polarization level is slightly degraded, Kraus, Fleisch [23].
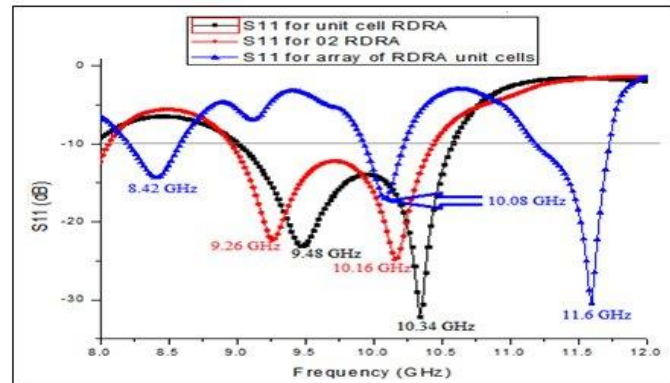


Fig. 3: Plot of Return loss versus Frequency
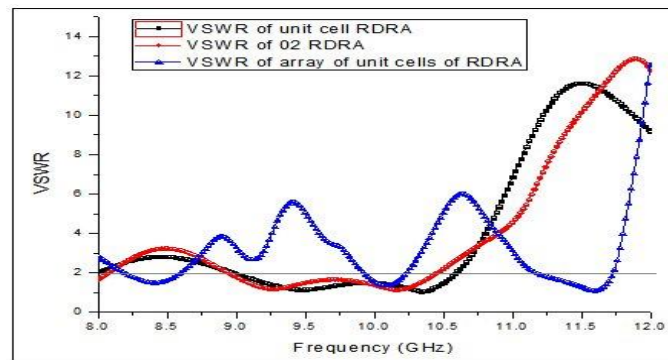


Fig. 4: Plot of VSWR versus Frequency

SOVAN MOHANTY, BAIBASWATA MOHAPATRA
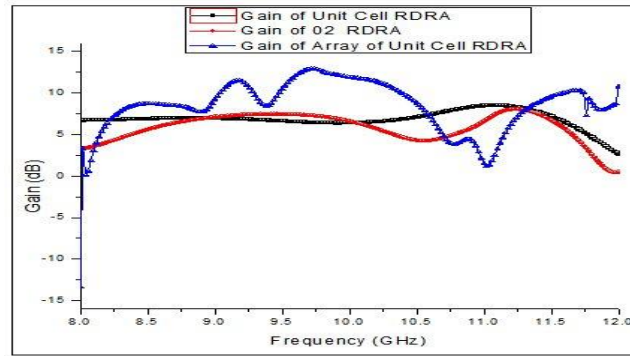


Fig. 5: Rectangular plot of Gain versus Frequency
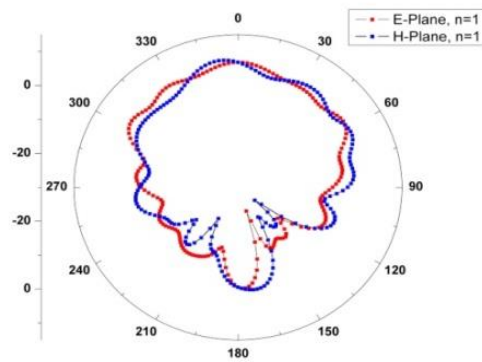


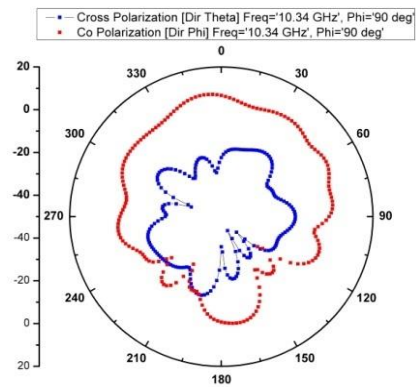Fig. 6a: E and H plane of the unit cell antenna (10dB/div) at 10.34 GHz



Fig. 6b: Radiation pattern indicating E-plane co and cross polarization of the antenna (Unit cell) (10 dB/div)
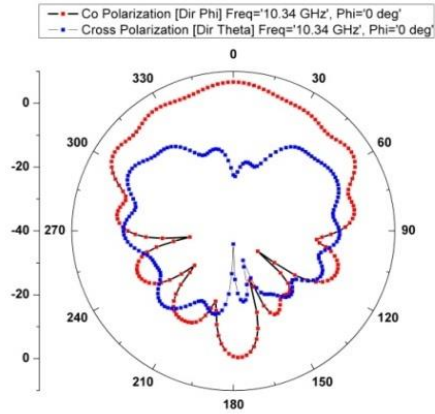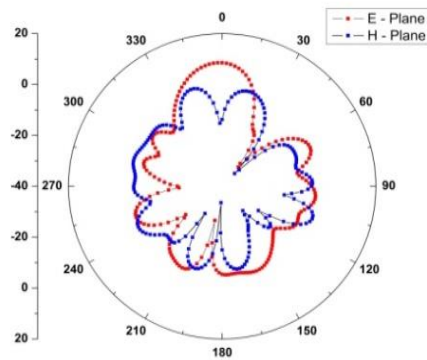
Fig. 6c: Radiation pattern indicating H-plane co and cross polarization of the antenna (Unit cell) (10 dB/div)



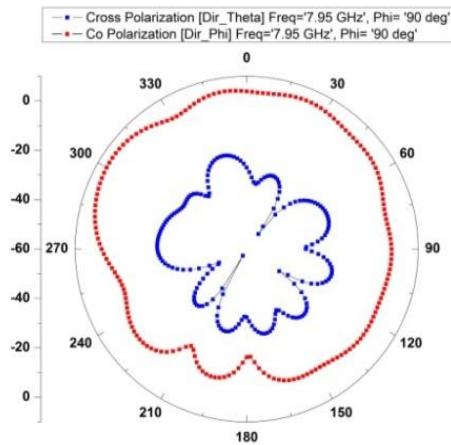Fig. 7a: E and H plane of the two cells antenna (10dB/div) at 7.95 GHz



Fig. 7b: Radiation pattern indicating E-plane co and cross polarization of the antenna (Two cells) (10 dB/div)
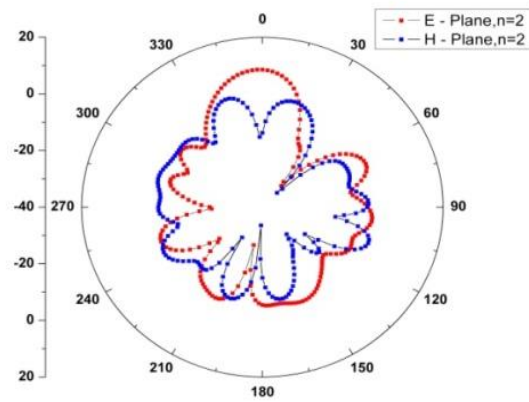
Fig. 7c: Radiation pattern indicating E-plane co and cross polarization of the antenna (Two cells)
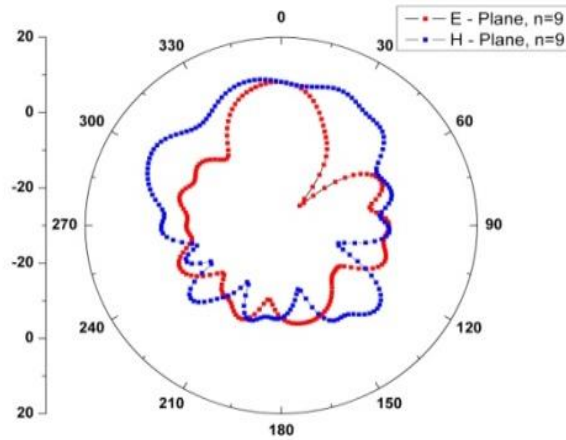


Fig. 8a: E and H plane of the nine cells antenna (10dB/div) at 7.95 GHz
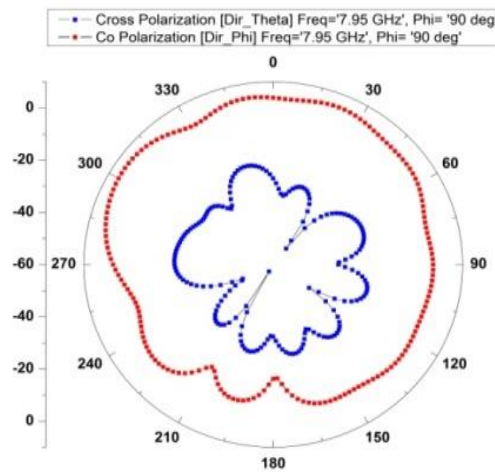


Fig. 8b: Radiation pattern indicating E-plane co and cross polarization of the antenna (Nine cells)    (10 dB/div)
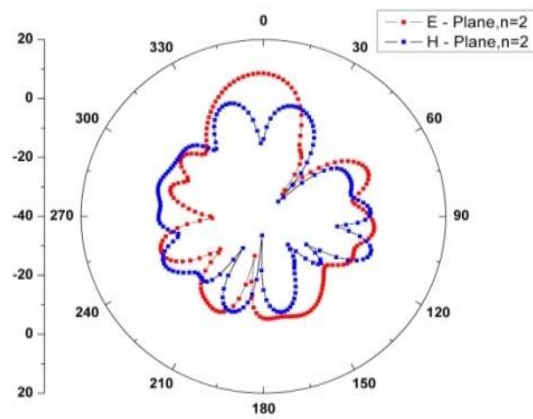
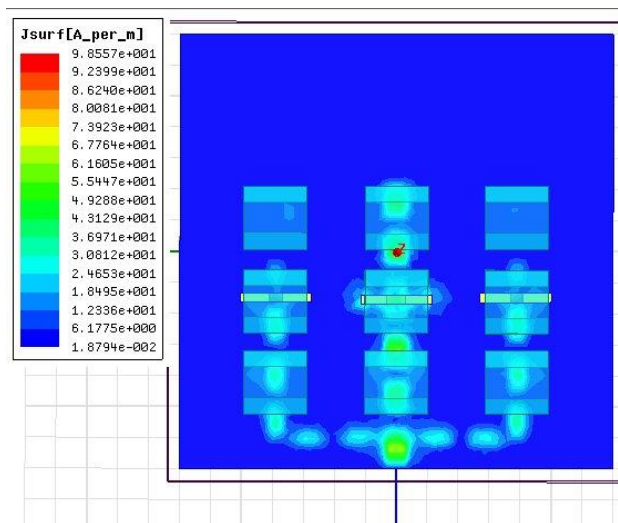Fig. 8c: radiation pattern indicating E-plane co and cross polarization of the antenna (Nine cells)



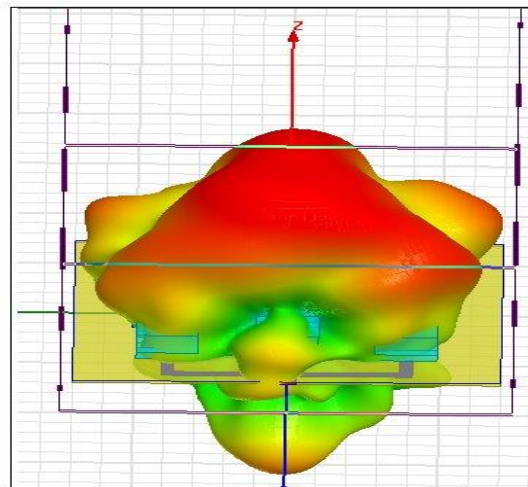Fig. 9: Distribution of current in the proposed antenna



Fig. 10: The broadside 3-D radiation pattern at 10.08 GHz on the x-y plane

**Table 2: A comparative analysis of parameters of three RDRA**

| Radiator | Impedance Band Width (%) | Peak Gain (dBi) | Resonating Frequency (GHz) | Radiation Efficiency (%) | Front to Back Ratio (FBR) (dB) |
|---|---|---|---|---|---|
| Unit Cell | 15.09 | 8.59 | 9.48, 10.34 | 96.47 | 12.22 |
| Double Cell | 14.56 | 8.08 | 9.26, 10.16 | 97.88 | 20.06 |
| 3×3 Array | 4.51,2.77,4.56 | 12.94 | 8.42,10.08,11.6 | 96.1 | 95.36 |

## 5. CONCLUSION

In this paper, VSWR, gain, and radiation patterns of the unit, double, and nine elements rectilinear dielectric slab are studied. For feeding, the aperture coupling method is used to produce radiation in the broadside direction. This RDRA array offers high design flexibility and satisfactory performance in achieving a high peak gain of 12.94 dBi with a relatively large and stable impedance bandwidth and low cross-polarization level less than 20 dB to that of co-polarization. The observed radiation efficiency of the array is 96.1% including the effect of back radiation. The performance of this array geometry can be improved by using stacked multi-segment DRA. It is required to solve rectilinear RDRA array with rigorous mathematical modeling to predict input impedance, coupling mechanisms, and radiation patterns.

## CONFLICT OF INTERESTS

The author(s) declare that there is no conflict of interests.

## REFERENCES

[1]   R. D. Richtinger, Dielectric resonator, J. Appl. Phys. 10 (1939), 391-398.

[2]   A. Okaya, L. F. Barash, The dielectric microwave resonator, Proc. IRE, 50 (1962), 2081-2092.

[3]   K. M. Luk, K. W. Leung, Dielectric resonator antennas. Baldock, Herefordshire: Research Studies Press, (2003).

[4]   A. Petosa, Dielectric resonator antenna handbook. Norwood: Artech house (2007).

[5]   A. Petosa, Design of microstrip-fed series array of dielectric resonator antennas, IEE Electron. Lett. 31 (1995), 1306-1307.

[6]  A. Petosa, Low profile phased array of dielectric resonator antennas, IEEE Int. Sympos. Phased Array Syst. Technol. (1996),182-185.

[7]  M. T. Hussain, M. S. Sharawi, S. Podilchack,Y. M. M. Antar, Closely packed millimeter wave MIMO antenna arrays with dielectric resonator elements, in 10th European Conference on Antenna and Propagation,(2016).

[8]  A. Petosa, Microstrip fed array of multi-segment dielectric resonator antenna, IEEE Proceeding-Microwave Antennas and Propagation, 144 (1997), 472-476.

[9]  B. B. Jones, F. Y. Chow, A. W. Sheeto, The synthesis of shaped patterns with series-fed microstrip patch arrays, IEEE Trans. Antennas Propagation, 30 (1982), 1206-1212.

[10] A. Petosa, S. Thirakoune, Rectangular dielectric resonator antenna with enhanced gain, IEEE Trans. Antennas Propagation, 59 (2011), 1385-1389.

[11] R. K. Mongia, P. Bhartia, Dielectric resonator antennas- a review and general design relations for resonant frequency and bandwidth, Int. J. Microwave Millimeter-Wave Computer-Aided Eng. 4 (1994), 230-247.

[12] R. F. Harrington, Time Harmonic Electromagnetic Fields, IEEE Press, (2001).

[13] G. D. Loos, Y. M. M. Antar, A new aperture coupled rectangular dielectric resonator antenna array, Microwave Optical Technol. Lett. 7 (1994), 642-644.

[14] A. Petosa, A. Ittipiboon, Y. M. M. Antar, D. Roscoe, M. Cuhaci, Recent advances in dielectric-resonator antenna technology, IEEE Antennas Propag. Mag. 40 (1998), 35–48.

[15] M. T. Birand, R. V. Gelsthrope, Experimental millimeter array using dielectric radiators fed by means of dielectric waveguides, Electron. Lett. 17 (1981), 633-635.

[16] S. Mohanty, B. Mohapatra, Leaky wave-guide based dielectric resonator antenna for millimeter-wave applications, Trans. Electr. Electron. Mater. 22 (2021), 310–316.

[17] T. H. Chang, Dualband split dielectric resonator antenna, IEEE Trans. Antennas Propag. 55 (2007), 3155-3161.

[18] R. K. Mongia, A. Ittipiboon, Theoretical and experimental investigations on rectangular dielectric resonator antennas, IEEE Trans. Antennas Propag. 45 (1997), 1348-1356.

[19] F. Wang, C. Zhang, H. Sun, Y. Xiao, Ultra wide band dielectric resonator antenna design based on multilayer form, Int. J. Antennas Propag. 2019 (2019), Article ID 4391474.

[20] Y. M. M. Anter, Z. Fan, Theoretical Investigation of Aperture-coupled rectangular dielectric resonator antenna,

IEEE Proc.- Microwave Antenna Propag. 143 (1996), 113-118.

[21] R. S. Yaduvanshi, H. Parthasarathy, Rectangular dielectric resonator antennas, theory, and design. Springer, (2016).

[22] N. A. Shalaby, S. E. Sherbiny, Mutual coupling reduction of DRA for MIMO applications, Adv. Electromagnetics, 8 (2019), 75–81.

[23] J. D. Kraus, D. A. Fleisch, Electromagnetics with applications, Tata Mc-GrawHill, (2010).